Nucleon-pair states of even-even Sn isotopes based on realistic effective interactions

Y. Y. Cheng,[1] C. Qi,[2] Y. M. Zhao,[1,3,*] and A. Arima[1,4]

[1]*Department of Physics and Astronomy, Shanghai Jiao Tong University, Shanghai 200240, China*

[2]*Department of Physics, Royal Institute of Technology (KTH), Stockholm SE-10691, Sweden*

[3]*IFSA Collaborative Innovation Center, Shanghai Jiao Tong University, Shanghai 200240, China*

[4]*Musashi Gakuen, 1-26-1 Toyotamakami Nerima-ku, Tokyo 176-8533, Japan*

(Received 25 December 2015; revised manuscript received 26 April 2016; published 15 August 2016)

In this paper we study yrast states of ^{128,126,124}Sn and ^{104,106,108}Sn by using the monopole-optimized realistic interactions in terms of both the shell model (SM) and the nucleon-pair approximation (NPA). For yrast states of ^{128,126}Sn and ^{104,106}Sn, we calculate the overlaps between the wave functions obtained in the full SM space and those obtained in the truncated NPA space, and find that most of these overlaps are very close to 1. Very interestingly, for most of these states with positive parity and even spin or with negative parity and odd spin, the SM wave function is found to be well represented by *one nucleon-pair basis state*, viz., a simple picture of "nucleon-pair states" (nucleon-pair configuration without mixings) emerges. In ^{128,126}Sn, the positive-parity (or negative-parity) yrast states with spin $J > 10$ (or $J > 7$) are found to be well described by breaking one or two S pairs in the 10^+_1 (or 7^-_1) state, i.e., the yrast state of seniority-two, spin-maximum, and positive-parity (or negative-parity), into non-S pair(s). Similar regularity is also pointed out for ^{104,106}Sn. The evolution of $E2$ transition rates between low-lying states in ^{128,126,124}Sn is discussed in terms of the seniority scheme.

DOI: 10.1103/PhysRevC.94.024321

I. INTRODUCTION

Sn isotopes provide the longest semimagic isotopic chain. From the proton-rich side, the enhanced $B(E2, 0^+_{\text{g.s.}} \to 2^+_1)$ values of even-even Sn isotopes with A from 104 to 114 have attracted much attention in the last decade (see, e.g., Refs. [1–13]). From the neutron-rich side, the level structures including the high-spin structure, as well as the electromagnetic properties, of even-even Sn nuclei with neutron holes inside the ^{132}Sn core, have also been extensively studied [14–24].

For semimagic nuclei, pair-truncation schemes of the shell model, such as the generalized seniority scheme [25–27] and broken pair model [28,29], provide us with proper frameworks. Although shell-model calculations for semimagic chains in light, middle, and middle-heavy mass regions are now well within the computer power, pair-truncation schemes are powerful to interpret shell-model results and provide a simple picture for semimagic nuclei. From the generalized seniority scheme, for even-even semimagic nuclei, the ground state can be represented by the collective-S-pair condensation, namely the seniority-zero state $|S^N\rangle$, and a few lowest excited states can be described by $(N-1)$ S pairs coupled to two unpaired nucleons, namely seniority-two states; here N is half of the valence nucleon number. In Refs. [30,31] it was shown that, for even-even Sn nuclei close to ^{100}Sn and those close to ^{132}Sn, the wave functions of the ground state and a few lowest excited states obtained in the full shell-model space well overlap with the wave functions of the seniority-zero and seniority-two states, respectively, based on effective interactions. For heavy Sn isotopes with a few neutrons outside ^{132}Sn, this simple picture also holds [32]. Recently, for the Ca isotopic chain, a systematic comparison between the shell-model results and those by using the generalized seniority scheme, with realistic interactions, was performed in Ref. [33], where it was shown that the energies, occupancies of single-j orbits, and electromagnetic observables of low-lying states, as well as their evolution with the neutron number, calculated in the low-dimensional seniority $v \leqslant 2$ space, were close to those in the full shell-model space.

In the nucleon-pair approximation (NPA) [34], by selecting only a few important collective non-S pairs, the degrees of freedom for unpaired nucleons in the generalized seniority scheme are further reduced. The wave function of a seniority-two state with given spin J and parity P is equivalent to a nucleon-pair basis state in the NPA, constructed by $(N-1)$ S pairs and one non-S pair with spin J and parity P (the structure coefficients of this non-S pair correspond to the wave function of this seniority-two state). For both the ground state and the excited states characterized by seniority two, a very simple picture mentioned above was pointed out in the generalized seniority works such as Refs. [30–33]. It is now interesting to ask whether this simple picture survives for states with larger seniority number. In this paper we extend this picture to seniority-four and seniority-six states.

In Ref. [35], monopole-optimized effective interactions for Sn isotopes were proposed by fitting to the binding energies of 157 low-lying yrast states of $^{102-132}$Sn. The interactions started from the realistic CD-Bonn nucleon-nucleon potential [36], and were renormalized by using the perturbative G-matrix approach [37]. It was also shown in Ref. [35] that, for low-lying yrast states up to 12^+_1 of the even-even Sn isotopic chain, the results given by the shell-model calculation with this set of effective interactions remarkably reproduce experimental data. One then expects this set of effective interactions to provide a satisfactory description also for positive-parity states with higher spins as well as negative-parity states of these Sn nuclei. Therefore we take this set of effective interactions in our present calculations, and study yrast states with positive parity or negative parity, for ^{128,126,124}Sn and ^{104,106,108}Sn, in

*Corresponding author: ymzhao@sjtu.edu.cn

both the full shell-model space and in the truncated NPA space. We calculate $B(E2)$ values and magnetic moments for the six nuclei, and study the evolution of $B(E2)$ values.

This paper is organized as follows. In Sec. II we introduce briefly the framework of the NPA, including the nucleon-pair basis and the shell-model Hamiltonian and observable operators. In Sec. III we present and discuss our calculated results for the above six even-even Sn isotopes, and in Sec. IV we summarize this paper.

II. THE NUCLEON-PAIR APPROXIMATION OF THE SHELL MODEL

The model space of the nucleon-pair approximation (NPA) is constructed by using both S and non-S pairs. If all possible nucleon pairs are considered, the NPA space is equivalent to the full shell-model space; if only a few important pairs are considered, the NPA space is much smaller than the exact shell-model space. The general framework of the NPA was proposed in Ref. [38] and refined in Refs. [39,40]. For a comprehensive review of the NPA formalism and its applications, see Ref. [34].

A. Nucleon-pair basis

In the NPA, the configuration space is constructed by using collective nucleon pairs defined as follows:

$$A^{r\dagger}|0\rangle = \sum_{ab} y(abr)A^{r\dagger}(ab)|0\rangle,$$
$$A^{r\dagger}(ab) = (C_a^\dagger \times C_b^\dagger)^r. \quad (1)$$

Here r is the spin of the collective pair, $C_a^\dagger$ is a creation operator for a nucleon in the a orbit, and $A^{r\dagger}(ab)$ is a creation operator of a noncollective pair with one nucleon in the a orbit and the other in the b orbit. The collective pair with spin r is represented by a linear combination of various noncollective pairs with spin r. $y(abr)$ is called the structure coefficient. For a system with $2N$ valence nucleons, a basis state is constructed by coupling N collective nucleon pairs successively,

$$((A^{r_1\dagger} \times A^{r_2\dagger})^{(J_2)} \times \cdots \times A^{r_N\dagger})^{(J_N)}|0\rangle. \quad (2)$$

In this work, the structure coefficients are obtained in the following procedures. We consider first the collective S pair, denoted by $S^\dagger = \sum_j y(jj0)(C_j^\dagger \times C_j^\dagger)^{(0)} = \sum_j y(jj0)S_j^\dagger$. The structure coefficients $y(jj0)$, with j running over all the single-particle orbits, are determined variationally, to minimize the energy functional $\langle S^N|H|S^N\rangle/\langle S^N|S^N\rangle$ [28]. As for collective non-S pairs, we diagonalize the Hamiltonian in the $(S^\dagger)^{(N-1)}A^{r\dagger}(j_1j_2)$ space ($S^\dagger$ is the collective pair with spin zero and $A^{r\dagger}(j_1j_2)$ is the noncollective pair with spin $r \neq 0$), with j_1, j_2 running over all the single-particle orbits. The lowest-state wave function is written in terms of $(S^\dagger)^{(N-1)}\sum_{j_1j_2} c(j_1j_2)A^{r\dagger}(j_1j_2)$, and we assume $y(j_1j_2r) = c(j_1j_2)$.

B. The shell model Hamiltonian and electromagnetic multipole operator

In this work the effective interactions are taken from Ref. [35], where the $T = 1$ matrix elements are monopole-optimized. The form of our Hamiltonian is as below:

$$H = \sum_\alpha \varepsilon_\alpha \hat{N}_\alpha + \frac{1}{4}\sum_{\alpha\beta\gamma\delta JT} \langle j_\alpha j_\beta|V|j_\gamma j_\delta\rangle_{JT} A^\dagger_{j_\alpha j_\beta JT} A_{j_\delta j_\gamma JT},$$

where ε_α is the single-particle energy, and $\langle j_\alpha j_\beta|V|j_\gamma j_\delta\rangle_{JT}$ is the two-body matrix elements. As in this work the calculation is performed for semimagic Sn isotopes, 160 two-body matrix elements with $T = 1$ are adopted.

In this work the reduced electric quadrupole transition probability for Sn isotopes is given by

$$B(E2) = \frac{1}{2J_i+1}(\alpha_f J_f \| e_\nu Q_\nu \| \alpha_i J_i)^2. \quad (3)$$

The one-body operator Q is defined as below:

$$Q = \sum_{jj'} q(jj'2)(C_j^+ \times \tilde{C}_{j'})^{(2)},$$
$$q(jj'2) = \frac{(j\|r^2Y^2\|j')}{\sqrt{5}}. \quad (4)$$

The magnetic dipole moment for Sn isotopes is given by

$$\mu = \sqrt{\frac{4\pi}{3}}\langle JM = J|g_{l\nu}L_\nu + g_{s\nu}S_\nu|JM = J\rangle. \quad (5)$$

The one-body operators L and S are defined as below:

$$L = \sum_{jj'} q_l(jj'1)(C_j^+ \times \tilde{C}_{j'})^{(1)},$$
$$S = \sum_{jj'} q_s(jj'1)(C_j^+ \times \tilde{C}_{j'})^{(1)},$$
$$q_l(jj'1) = \delta_{ll'}(-1)^{l+1/2+j'}\sqrt{\frac{l(l+1)}{3}}\hat{j}\hat{j}'\hat{l}\begin{Bmatrix} j & j' & 1 \\ l' & l & \frac{1}{2}\end{Bmatrix},$$
$$q_s(jj'1) = \delta_{ll'}(-1)^{l+1/2+j}\frac{1}{\sqrt{2}}\hat{j}\hat{j}'\begin{Bmatrix} j & j' & 1 \\ \frac{1}{2} & \frac{1}{2} & l\end{Bmatrix}. \quad (6)$$

For the definition of the reduced matrix element, see Eq. (8.4) of Ref. [27].

III. RESULTS AND DISCUSSIONS

A. ^{128,126,124}Sn

For ^{128,126,124}Sn, we perform three sets of calculation within the framework of the nucleon-pair approximation, with our focus on the yrast states with positive parity or negative parity, including those with high spins. The first set (denoted as "SM") is performed in the full shell-model configuration space, which is realized in the NPA by considering all possible nucleon pairs. The second set (denoted as "NPA") is performed in the nucleon-pair truncated space, by considering only a few collective S and non-S pairs. In the third set (denoted as "pair state"), the configuration space of each state is constructed by *the one-dimensional, optimized pair basis state* in the form of Eq. (2), i.e., a simple configuration assuming no mixings with

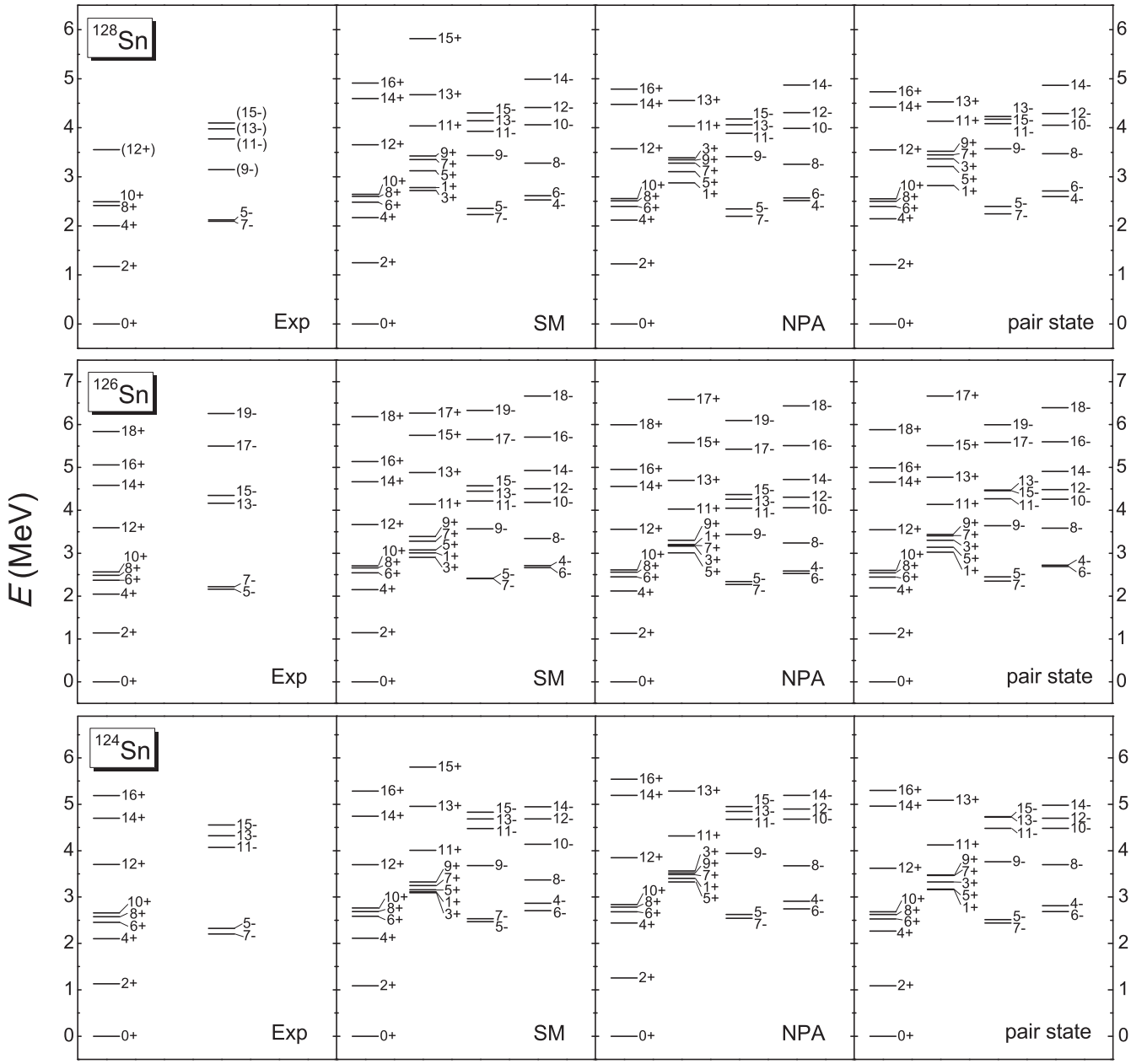

FIG. 1. Energy levels of yrast states for ^{128,126,124}Sn obtained in three sets of calculations by using the monopole-optimized effective interactions based on the realistic CD-Bonn nucleon-nucleon potential, in comparison with experimental data. The first set (denoted as "SM") is performed in the full shell-model configuration space. In the second set (denoted as "NPA"), the configuration space for positive parity is constructed by using collective positive-parity pairs with spin zero, two, four, six, eight, and ten; the configuration space for negative parity is constructed by coupling the above positive-parity pairs to one negative-parity pair with spin four, five, six, and seven, respectively. In the third set (denoted as "pair state"), the configuration space for a given spin and parity is constructed by the one-dimensional, optimized nucleon-pair basis state. In the NPA calculation for ^{124}Sn, up to two non-S pairs are considered in the nucleon-pair truncated subspace. The experimental data is taken from Refs. [16,17].

other basis states. In this work, the optimized pair basis state is the largest component of corresponding NPA wave function for each yrast state.

In our NPA calculation (i.e., the second set denoted by "NPA"), the configuration space of positive parity is constructed by using collective pairs with positive parity and even spin, i.e., positive-parity pairs with spin zero, two, four, six, eight, and ten, denoted as S, D, G, I, K, M, respectively. For the yrast $J^P = 1^+$ state which is essentially a seniority-two state, we further consider the seniority-two configuration $|S^{(N-1)}P\rangle$ (P denotes the positive-parity spin-one pair). Because neutron holes predominantly occupy the $s_{1/2}$, $d_{3/2}$, and $h_{11/2}$ orbits in the low-lying states of ^{128,126,124}Sn, the spins of our negative-parity pairs are between four and seven. Our configuration space of negative-parity states is constructed by coupling the adopted positive-parity even-spin nucleon pairs to one

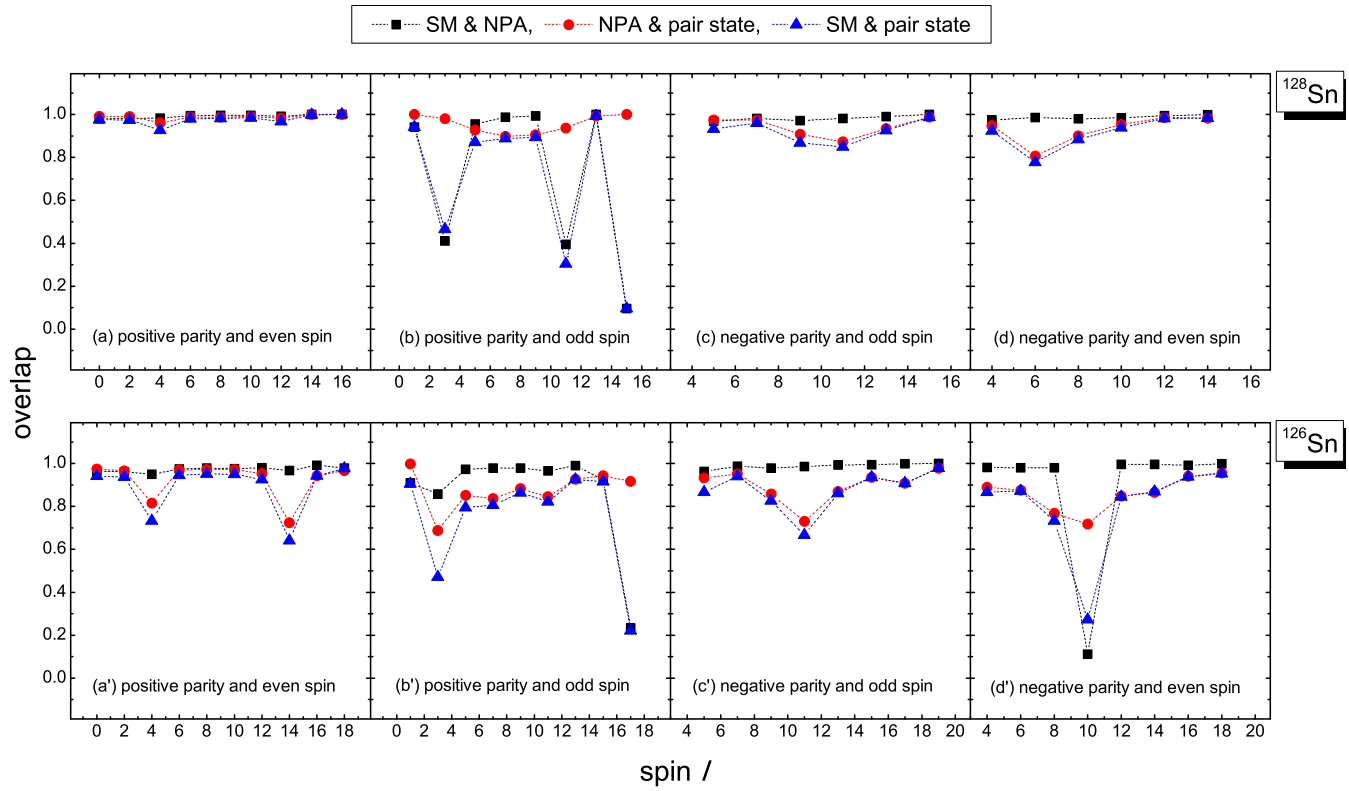

FIG. 2. For the yrast states of ^{128,126}Sn, the overlap between the SM wave function and corresponding NPA wave function (solid black squares), the overlap between the NPA wave function and corresponding one-dimensional, optimized pair basis state (solid red circles), and the overlap between the SM wave function and the optimized pair basis state (solid blue up-triangles). (a) and (a′) [(b) and (b′), (c) and (c′), (d) and (d′)] correspond to the yrast states with positive parity and even spin [positive parity and odd spin, negative parity and odd spin, negative parity and even spin] for ^{128}Sn and ^{126}Sn, respectively.

negative-parity nucleon pair with spin four, five, six, and seven, denoted as $\mathcal{G}$,$\mathcal{H}$,$\mathcal{I}$, and $\mathcal{J}$, respectively.

In Fig. 1 we present calculated energy levels of ^{128,126,124}Sn in the above three sets of configuration spaces, in comparison with experimental data. One sees both the positive-parity yrast states with $J > 12$ and the negative-parity yrast states are very well described in the full SM space. One also sees that the energy levels of the NPA calculation are almost the same as those obtained in the full SM space, with very few exceptions. Very interestingly, the energy levels calculated by using one-dimensional, optimized nucleon-pair basis states (to be tabulated below) are also close to the results of the SM calculation, with very few exceptions.

It is therefore very interesting to investigate wave functions obtained in these three sets of calculations. In Fig. 2, for each yrast state of ^{128}Sn and ^{126}Sn, we present the overlap between the SM wave function and corresponding NPA wave function, the overlap between the NPA wave function and corresponding one-dimensional, optimized nucleon-pair basis state, and the overlap between the SM wave function and the optimized nucleon-pair basis state. One sees the overlaps between those SM wave functions and corresponding NPA wave functions (solid black squares) are very close to 1 (except for the 3^+_1 and 11^+_1 states of ^{128}Sn and the 10^-_1 state of ^{126}Sn). This means that for these yrast states the SM wave functions are well approximated by the wave functions obtained in a much smaller, truncated subspace constructed by collective nucleon pairs. Because the NPA wave functions are well approximated by the optimized nucleon-pair basis states (as shown in Fig. 2), the overlaps between the SM wave functions and corresponding nucleon-pair basis states (solid blue up-triangles) are very large (>0.8). Therefore we call these states simply "pair states", to stress the simplicity of these low-lying states in terms of collective nucleon pairs.

In Tables I and II, we present the yrast states of ^{128}Sn and ^{126}Sn in terms of their pair states, with the requirement that the overlaps of these nucleon-pair basis states with corresponding SM wave functions are larger than 0.8. Many of these yrast states, e.g., the yrast positive-parity states with spin $J > 10$ and negative-parity states with spin $J > 7$, are well described by two or three non-S pairs. This means that the generalized seniority is a good quantum number, and that *each of these seniority-four or seniority-six states can be further reduced to an extremely simple, one-dimensional nucleon-pair basis state, constructed by two or three collective non-S pairs, within a good accuracy*.

According to Table I, the positive-parity yrast states with spin $J > 10$ are given by a nucleon-pair basis state of one M (spin-ten and positive-parity) pair and another positive-parity non-S pair, and the negative-parity yrast states with spin $J > 7$ are given by a nucleon-pair basis state of one $\mathcal{J}$ (spin-seven and negative-parity) pair and one positive-parity

TABLE I. One-dimensional, optimized nucleon-pair basis state, for which the overlap with corresponding SM wave function is larger than 0.8, and the dimensions of corresponding SM and NPA configuration spaces, for the yrast states of the ^{128}Sn nucleus. S,D,G,I,K,M, and P represent positive-parity nucleon pairs with spin $J = 0,2,4,6,8,10$, and 1, respectively. $\mathcal{G},\mathcal{H},\mathcal{I},\mathcal{J}$ correspond to negative-parity nucleon pairs with spin $J = 4,5,6,7$, respectively.

J^P	dimension		pair
	SM	NPA	state
0_1^+	50	6	$\|S^2\rangle$
2_1^+	166	10	$\|SD\rangle$
4_1^+	197	13	$\|SG\rangle$
6_1^+	161	14	$\|SI\rangle$
8_1^+	114	14	$\|SK\rangle$
10_1^+	71	12	$\|SM\rangle$
12_1^+	37	8	$\|DM\rangle$
14_1^+	13	4	$\|GM\rangle$
16_1^+	3	2	$\|IM\rangle$
1_1^+	90	1	$\|SP\rangle$
5_1^+	165	7	$\|DG\rangle$
7_1^+	121	8	$\|DI\rangle$
9_1^+	80	8	$\|DM\rangle$
13_1^+	20	4	$\|IK\rangle$
			$\|IM\rangle$
			$\|KM\rangle$
15_1^+	4	1	$\|IM\rangle$
5_1^-	175	20	$\|S\mathcal{H}\rangle$
7_1^-	162	20	$\|S\mathcal{J}\rangle$
9_1^-	103	16	$\|D\mathcal{J}\rangle$
11_1^-	47	12	$\|G\mathcal{J}\rangle$
13_1^-	16	8	$\|M\mathcal{J}\rangle$
15_1^-	4	4	$\|K\mathcal{J}\rangle$
			$\|M\mathcal{J}\rangle$
4_1^-	160	18	$\|S\mathcal{G}\rangle$
8_1^-	135	18	$\|D\mathcal{J}\rangle$
10_1^-	73	14	$\|G\mathcal{J}\rangle$
12_1^-	27	10	$\|K\mathcal{J}\rangle$
14_1^-	8	6	$\|M\mathcal{J}\rangle$

non-S pair. From this perspective, the yrast positive-parity states with $J > 10$ and negative-parity states with $J > 7$ can be regarded as excited states with respect to the 10_1^+ and 7_1^- states, respectively, which are the seniority-two spin-maximum yrast state with positive parity or negative parity; for example, the 10_1^+ state is given dominantly by $|SM\rangle$ and the 12_1^+ state by $|DM\rangle$, therefore the 12_1^+ state can be regarded as an excitation of the 10_1^+ state by breaking the S pair into the D pair. The situation of the ^{126}Sn nucleus is very similar, as shown in Table II.

In Tables I and II, one also sees a few low-lying yrast states are represented alternatively by several pair basis states, for example, the 18_1^+ state of ^{126}Sn is well approximated by either the $|r_1r_2r_3,J_2\rangle = |DKK,10\rangle$ or $|DIM,8\rangle$ basis state. This is originated from the nonorthogonality of the nucleon-pair basis; in other words, the overlap of these two pair basis states is very large.

TABLE II. Same as in Table I except for the ^{126}Sn nucleus. For the pair states with three non-S pairs, we denote $((A^{r_1\dagger} \times A^{r_2\dagger})^{(J_2)} \times A^{r_3\dagger})^{(J_3)}|0\rangle$ by using $|r_1r_2r_3,J_2\rangle$ without confusion. J_3 is suppressed, and J_2 is also suppressed in the case of $r_1 = 0$.

J^P	dimension		pair
	SM	NPA	state
0_1^+	518	33	$\|S^3\rangle$
2_1^+	2134	85	$\|S^2D\rangle$
6_1^+	3170	161	$\|S^2I\rangle$
8_1^+	2715	149	$\|S^2K\rangle$
10_1^+	2000	134	$\|S^2M\rangle$
12_1^+	1255	92	$\|SDM\rangle$
16_1^+	258	39	$\|SKK\rangle$
			$\|SIM\rangle$
18_1^+	77	17	$\|DKK,10\rangle$
			$\|DIM,8\rangle$
1_1^+	1281	32	$\|S^2P\rangle$
7_1^+	2919	137	$\|SDI\rangle$
9_1^+	2320	97	$\|SDM\rangle$
11_1^+	1576	106	$\|SDM\rangle$
13_1^+	897	80	$\|SIK\rangle$
			$\|SIM\rangle$
			$\|SKM\rangle$
15_1^+	406	46	$\|DIM,6\rangle$
5_1^-	3151	373	$\|S^2\mathcal{H}\rangle$
7_1^-	3098	398	$\|S^2\mathcal{J}\rangle$
9_1^-	2444	366	$\|SD\mathcal{J}\rangle$
13_1^-	853	188	$\|SM\mathcal{J}\rangle$
15_1^-	389	125	$\|SK\mathcal{J}\rangle$
17_1^-	145	67	$\|IK\mathcal{I},12\rangle$
			$\|IK\mathcal{J},11\rangle$
			$\|GM\mathcal{J},11\rangle$
19_1^-	41	27	$\|IK\mathcal{J},13\rangle$
			$\|IM\mathcal{J},13\rangle$
4_1^-	2896	330	$\|S^2\mathcal{G}\rangle$
6_1^-	3221	394	$\|S^2\mathcal{I}\rangle$
12_1^-	1185	232	$\|SK\mathcal{J}\rangle$
14_1^-	584	151	$\|SM\mathcal{H}\rangle$
			$\|SK\mathcal{I}\rangle$
			$\|SK\mathcal{J}\rangle$
16_1^-	243	86	$\|DM\mathcal{H},11\rangle$
			$\|DK\mathcal{J},10\rangle$
18_1^-	81	36	$\|KM\mathcal{H},13\rangle$
			$\|II\mathcal{J},12\rangle$

In Table III we present the calculated $B(E2)$ values and magnetic moments of ^{128,126,124}Sn, obtained in the three sets of configuration spaces, namely "SM", "NPA", and "pair state", and compare them with experimental data. The effective charge for neutron holes is taken to be $e_\nu = -0.88e$, as in Ref. [35], and the orbital and spin gyromagnetic ratios for neutron holes $g_{l\nu}$ and $g_{s\nu}$ are taken to be 0 and $-3.826 \times 0.7\mu_N$, respectively. The oscillator parameter is set as $r_0^2 = 1.012A^{1/3}$ fm^2. Because the overlaps between the SM wave functions and corresponding NPA wave functions (shown in Fig. 2) are close to 1 for most yrast states of

TABLE III. Calculated $B(E2)$ (in units of W.u.) and magnetic moments (in units of μ_N) of ^{128,126,124}Sn in three configuration spaces, namely "SM", "NPA", and "pair state" (denoted as "PS" for short), in comparison with experimental data taken from Refs. [14,20,21,24,41]. The effective charge of neutron holes is taken to be $-0.88e$ [35], and $g_{l\nu} = 0\mu_N$ and the quenched $g_{s\nu} = -3.826 \times 0.7\mu_N$ are adopted.

	^{128}Sn				^{126}Sn				^{124}Sn			
	Exp	SM	NPA	PS	Exp	SM	NPA	PS	Exp	SM	NPA	PS
$B(E2)$ (W.u.)												
$2_1^+ \to 0_1^+$	3.8(4)	4.43	4.23	3.94	5.4(16)	6.71	6.33	5.37	8.06(82)	8.46	7.36	6.31
$4_1^+ \to 2_1^+$	–	3.38	2.71	1.15	–	6.99	5.25	0.53	4.8(6)	11.46	2.77	0.14
$6_1^+ \to 4_1^+$	–	1.25	1.11	0.90	–	0.25	0.18	0.33	–	1.18	0.21	0.03
$8_1^+ \to 6_1^+$	–	0.91	0.85	0.57	–	0.70	0.40	0.20	–	0.29	0.02	0.01
$10_1^+ \to 8_1^+$	0.346(18)	0.42	0.37	0.21	0.15(1)	0.31	0.16	0.08	0.024(3)	<0.01	0.01	0.01
$12_1^+ \to 10_1^+$	–	2.71	2.74	2.47	–	5.75	5.60	4.42	–	7.89	4.94	5.73
$14_1^+ \to 12_1^+$	–	1.60	1.71	1.87	–	7.32	6.39	0.82	–	11.53	0.26	0.20
$16_1^+ \to 14_1^+$	–	1.22	1.22	1.23	–	0.04	<0.01	0.40	–	1.56	0.03	0.03
$18_1^+ \to 16_1^+$	–	–	–	–	–	2.15	2.07	2.45	–	–	–	–
$7_1^- \to 5_1^-$	–	0.70	1.21	0.84	0.29(7)	0.40	0.83	0.51	0.107(18)	0.04	1.11	0.29
$9_1^- \to 7_1^-$	–	2.31	2.06	1.82	–	4.27	4.04	3.24	–	6.22	4.50	4.14
$11_1^- \to 9_1^-$	–	3.77	3.15	1.86	–	4.05	3.57	0.72	–	0.87	0.14	0.10
$13_1^- \to 11_1^-$	–	3.58	3.08	1.40	–	0.16	0.06	0.55	–	3.04	0.27	0.07
$15_1^- \to 13_1^-$	–	2.26	2.23	1.25	–	1.93	1.93	0.52	–	0.05	0.23	0.12
$17_1^- \to 15_1^-$	–	–	–	–	–	3.36	3.48	1.09	–	–	–	–
$19_1^- \to 17_1^-$	–	–	–	–	–	2.80	2.82	2.01	–	–	–	–
μ (μ_N)												
2_1^+	−0.46(12)	−0.272	−0.327	−0.320	−0.24(6)	−0.254	−0.291	−0.297	−0.212(26)	−0.253	−0.280	−0.274
4_1^+	–	−0.837	−0.908	−0.915	–	−0.735	−0.837	−0.912	–	−0.652	−0.895	−0.903
6_1^+	–	−1.434	−1.456	−1.456	–	−1.416	−1.456	−1.457	–	−1.394	−1.456	−1.457
8_1^+	–	−1.934	−1.947	−1.948	–	−1.905	−1.943	−1.948	–	−1.884	−1.945	−1.948
10_1^+	–	−2.424	−2.432	−2.435	–	−2.387	−2.427	−2.435	–	−2.357	−2.430	−2.435
12_1^+	–	−2.665	−2.678	−2.743	–	−2.514	−2.653	−2.718	–	−2.436	−2.644	−2.688
14_1^+	–	−3.340	−3.341	−3.341	–	−2.931	−3.133	−3.337	–	−2.716	−3.292	−3.322
16_1^+	–	−3.891	−3.891	−3.889	–	−3.867	−3.886	−3.896	–	−3.755	−3.892	−3.889
18_1^+	–	–	–	–	–	−4.037	−4.193	−4.090	–	–	–	–

^{128,126}Sn, corresponding $B(E2)$ and μ values given by the NPA calculation are close to those given by the SM calculation, as expected.

In Tables I and II, one finds that the yrast states of ^{128,126}Sn with positive parity and spin below 17 (with an exception of the 15_1^+ state in ^{126}Sn), and those with negative parity

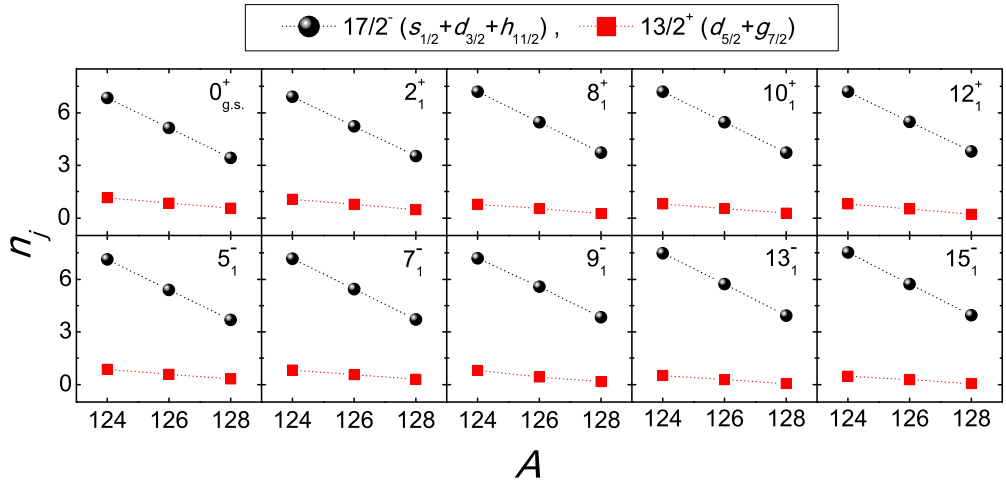

FIG. 3. The neutron-hole occupation number of the pseudo "$13/2^+$" and "$17/2^-$" shells for the 0_1^+, 2_1^+, 8_1^+, 10_1^+, 12_1^+, 5_1^-, 7_1^-, 9_1^-, 13_1^-, 15_1^- states versus mass number A, based on the SM calculation.

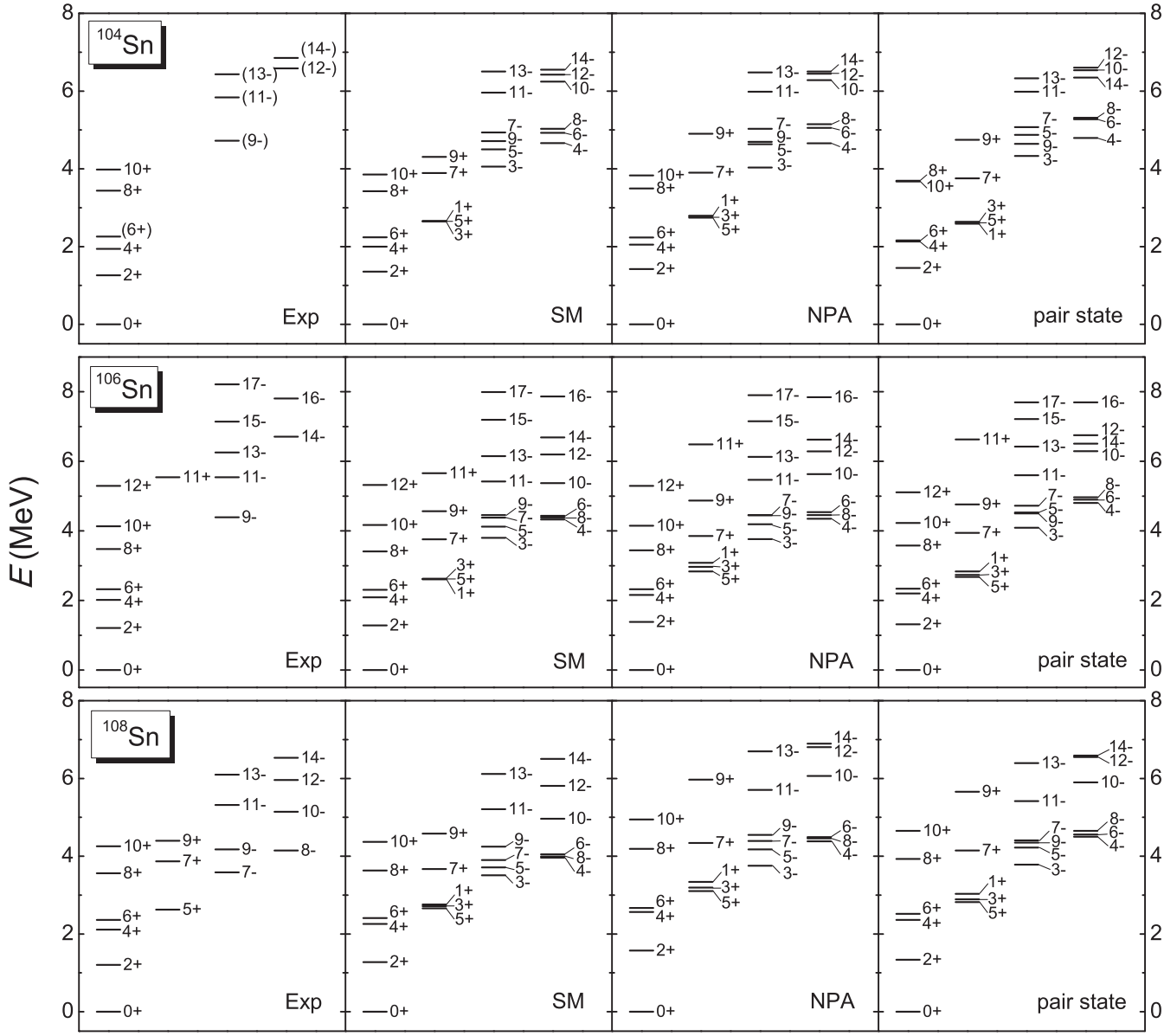

FIG. 4. Same as Fig. 1 except for ^{104,106,108}Sn and experimental data are taken from Ref. [41]. The building blocks of the NPA space include positive-parity pairs with spin zero, two, four, six, and negative-parity nucleon pairs with spin three, four, five, six, seven, eight, and nine. For ^{108}Sn, the maximum number for non-S pairs of each pair basis is limited to be two.

and spin below 16, are well represented by pair basis states with seniority up to four. This encourages us to simplify our calculation of ^{124}Sn by considering up to seniority-four configurations. This assumption is also justified by following results: from Fig. 1 and Table III, one sees that the NPA calculation considering up to two non-S pairs reasonably reproduces the energy levels and the general patterns of the electromagnetic properties given by the SM calculation.

In Ref. [11], the $B(E2,0^+_{\rm g.s.} \to 2^+_1)$ values for the Sn isotopic chain have been studied in terms of the generalized seniority scheme. The low-lying single-particle orbits, $\nu g_{7/2}$ and $\nu d_{5/2}$, were simplified as a single $j^\pi = 13/2^+$ shell, and the other three single-particle orbits, $\nu s_{1/2}, \nu d_{3/2}$, and $\nu h_{11/2}$, were simplified as a $j^\pi = 17/2^-$ orbit [11]. Under such an assumption, valence neutrons occupy the $13/2^+$ shell for low-lying states of Sn isotopes below ^{114}Sn, and neutron holes occupy the $17/2^-$ shell for low-lying states of Sn isotopes above ^{116}Sn, thus the $B(E2,0^+_{\rm g.s.} \to 2^+_1)$ values have two local maximum where the $13/2^+$ and $17/2^-$ shells are half-filled, respectively, and have a shallow minimum around ^{116}Sn. In Fig. 3 we present the neutron-hole occupation number of the $\nu s_{1/2}, \nu d_{3/2}$ and $\nu h_{11/2}$ orbits (the pseudo-"$17/2^-$" orbit of Ref. [11]), and the occupation number of $\nu g_{7/2}$ and $\nu d_{5/2}$ (the pseudo-"$13/2^+$" orbit), in the SM wave functions of the $0^+_1, 2^+_1, 8^+_1, 10^+_1, 12^+_1, 5^-_1, 7^-_1, 9^-_1, 13^-_1, 15^-_1$ states, versus mass number A. One sees for these low-lying yrast states of the three isotopes, as expected, neutron holes predominantly occupy the "$17/2^-$" shell. One also sees as mass number A decreases,

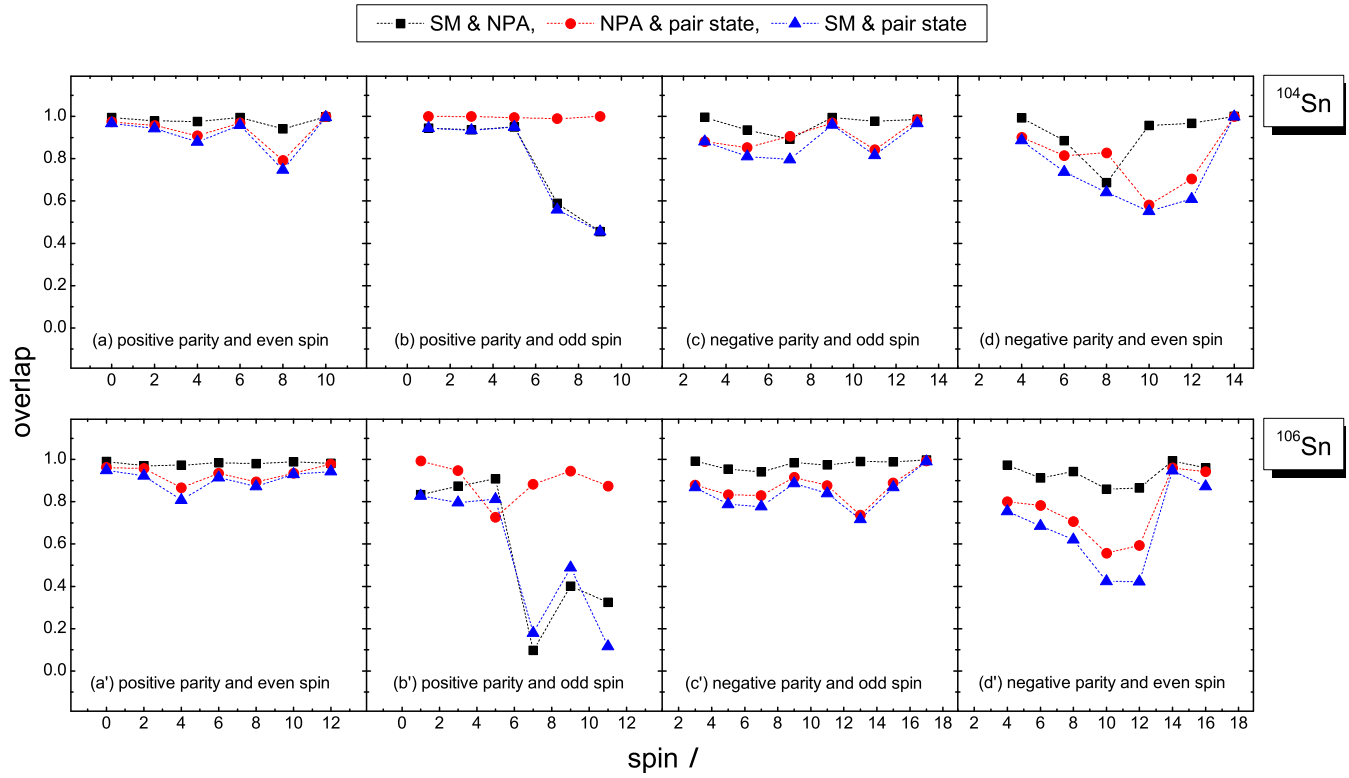

FIG. 5. Same as Fig. 2 except that the overlaps here are for the ^{104,106}Sn nuclei.

more and more neutron holes occupy the "$17/2^-$" shell which is close to half-filled at ^{124}Sn.

According to Tables I and II, the 0_1^+ and 2_1^+ states, the 10_1^+ and 12_1^+ states, the 7_1^- and 9_1^- states have seniority numbers differing by two, while the 8_1^+ and 10_1^+ states, the 5_1^- and 7_1^- states, the 13_1^- and 15_1^- states have the same seniority numbers. It is therefore expected that, according to the seniority scheme [27], qualitatively, the $B(E2)$ values of the seniority-changed $2_1^+ \to 0_1^+, 12_1^+ \to 10_1^+, 9_1^- \to 7_1^-$ transitions increase as mass number A decreases, while the $B(E2)$ values of the seniority-conserved $10_1^+ \to 8_1^+, 7_1^- \to 5_1^-, 15_1^- \to 13_1^-$ transitions decrease and nearly vanish at ^{124}Sn. Indeed the calculated $B(E2)$ values of these transitions given by the SM calculation evolve in this pattern.

B. ^{104,106,108}Sn

For ^{104,106,108}Sn, we also perform three sets of calculations, i.e., the "SM", "NPA", and "pair state" calculations, by using effective interactions of Ref. [35]. For the low-lying positive-parity states of these nuclei, valence neutrons predominantly occupy the $g_{7/2}$ and $d_{5/2}$ orbits, and correspondingly we adopt positive-parity neutron pairs with spin zero, two, four, and six, denoted as S, D, G, I, respectively; for negative-parity levels, the NPA space is constructed by coupling the above positive-parity pairs to one negative-parity neutron pair with spin three, four, five, six, seven, eight, and nine, denoted as $\mathcal{F}, \mathcal{G}, \mathcal{H}, \mathcal{I}, \mathcal{J}, \mathcal{K}$, and $\mathcal{L}$, respectively. Because the yrast states of $J^P = 1^+, 3^+, 5^+$ are expected to be seniority-two states, the seniority-two configurations $|S^{(N-1)}P\rangle, |S^{(N-1)}F\rangle$, and $|S^{(N-1)}H\rangle$ (P, F, H denote the positive-parity neutron pairs with spin one, three, and five, respectively) are also considered in our calculation of these three yrast states. Similar

TABLE IV. Same as in Table I except for ^{104}Sn. S, D, G, I and P, F, H denote positive-parity neutron pairs with spin $J = 0,2,4,6$ and 1,3,5, respectively. $\mathcal{F}$, $\mathcal{G}$, $\mathcal{H}$, $\mathcal{I}$, $\mathcal{J}$, $\mathcal{K}$, and $\mathcal{L}$ represent negative-parity pairs with spin $J = 3,4,5,6,7,8$, and 9, respectively.

J^P	dimension		pair
	SM	NPA	state
0_1^+	50	4	$\|S^2\rangle$
2_1^+	166	6	$\|SD\rangle$
4_1^+	197	7	$\|SG\rangle$
6_1^+	161	6	$\|SI\rangle$
10_1^+	71	2	$\|II\rangle$
1_1^+	90	1	$\|SP\rangle$
3_1^+	166	3	$\|SF\rangle$
5_1^+	165	4	$\|SH\rangle$
3_1^-	130	16	$\|I\mathcal{L}\rangle$
5_1^-	175	20	$\|S\mathcal{H}\rangle$
7_1^-	162	20	$\|S\mathcal{J}\rangle$
9_1^-	103	16	$\|S\mathcal{L}\rangle$
11_1^-	47	9	$\|D\mathcal{L}\rangle$
13_1^-	16	4	$\|I\mathcal{L}\rangle$
4_1^-	160	18	$\|I\mathcal{L}\rangle$
14_1^-	8	2	$\|I\mathcal{K}\rangle$
			$\|I\mathcal{L}\rangle$

TABLE V. Same as in Table IV except for the ^{106}Sn nucleus.

J^P	dimension		pair
	SM	NPA	state
0_1^+	518	13	$\|S^3\rangle$
2_1^+	2134	27	$\|S^2D\rangle$
4_1^+	3053	37	$\|S^2G\rangle$
6_1^+	3170	38	$\|S^2I\rangle$
8_1^+	2715	29	$\|SDI\rangle$
10_1^+	2000	20	$\|GII,6\rangle$
12_1^+	1255	12	$\|GII,8\rangle$
			$\|III,6\rangle$
			$\|III,8\rangle$
1_1^+	1281	8	$\|S^2P\rangle$
3_1^+	2602	23	$\|S^2F\rangle$
5_1^+	3110	27	$\|S^2H\rangle$
3_1^-	2455	168	$\|S^2\mathcal{F}\rangle$
9_1^-	2444	195	$\|S^2\mathcal{L}\rangle$
11_1^-	1577	141	$\|SD\mathcal{L}\rangle$
15_1^-	389	43	$\|DG\mathcal{L},6\rangle$
17_1^-	145	17	$\|GI\mathcal{J},10\rangle$
			$\|II\mathcal{J},10\rangle$
			$\|GG\mathcal{L},8\rangle$
14_1^-	584	61	$\|SI\mathcal{K}\rangle$
			$\|SI\mathcal{L}\rangle$
16_1^-	243	27	$\|DI\mathcal{K},8\rangle$
			$\|DI\mathcal{L},7\rangle$
			$\|DI\mathcal{L},8\rangle$

to the case of ^{124}Sn, we consider up to two non-S pairs in the NPA calculation of ^{108}Sn.

In Fig. 4 we present experimental energy levels and our calculated results of ^{104,106,108}Sn obtained in the above three sets of configuration spaces. One sees that these SM, NPA calculations provide us with a satisfactory description of yrast states with positive parity or negative parity. The simple picture of optimized nucleon-pair basis states also presents a good reproduction of the energy levels obtained in the SM calculations.

In Fig. 5 we present overlaps between the SM wave functions and corresponding NPA wave functions, overlaps between the NPA wave functions and corresponding optimized pair basis states, and overlaps between the SM wave functions and the optimized pair basis states, for yrast states of ^{104}Sn and ^{106}Sn. One sees that the overlaps between the SM wave functions and corresponding NPA wave functions are close to 1, with exceptions of the 7_1^+,9_1^+, and 8_1^- states of ^{104}Sn, and the 7_1^+,9_1^+, and 11_1^+ states of ^{106}Sn. This means the SM wave functions of most yrast states for ^{104,106}Sn can be well approximated by the wave functions obtained in our truncated space constructed by a few collective neutron pairs. In Fig. 5 one also sees for the yrast states with positive parity and even spin, as well as the yrast states with negative parity and odd spin, the SM wave functions well overlap with corresponding optimized pair basis states. This demonstrate once again the simple picture of optimized pair-basis states for these yrast states.

TABLE VI. Same as in Table III except for the ^{104,106,108}Sn nuclei. The effective charge for valence neutrons is taken as the opposite of that for neutron holes, namely $e_\nu = 0.88e$; the orbital and spin gyromagnetic ratios for valence neutrons are the same as those for neutron holes. Experimental data are taken from Refs. [4,8,41].

	^{104}Sn				^{106}Sn				^{108}Sn			
	Exp	SM	NPA	PS	Exp	SM	NPA	PS	Exp	SM	NPA	PS
$B(E2)$ (W.u.)												
$2_1^+ \to 0_1^+$	11.9(19)	4.69	4.33	3.92	13.1(26)	6.53	6.04	5.19	14.5(12)	7.45	6.65	6.09
$4_1^+ \to 2_1^+$	–	4.37	3.65	1.10	–	4.09	2.89	0.45	–	0.11	0.08	0.11
$6_1^+ \to 4_1^+$	4.2(15)	1.55	1.28	0.68	3.1(7)	0.03	<0.01	0.22	2.43(14)	0.30	0.03	0.05
$8_1^+ \to 6_1^+$	>0.6	1.97	1.89	0.11	–	4.91	4.42	2.93	0.107(15)	4.27	3.24	3.59
$10_1^+ \to 8_1^+$	4.1(6)	3.36	2.92	1.47	6.4(11)	3.65	3.33	1.28	–	1.61	0.02	0.01
$12_1^+ \to 10_1^+$	–	–	–	–	–	2.72	2.69	3.21	–	–	–	–
$5_1^- \to 3_1^-$	–	2.62	2.40	0.46	–	0.29	0.39	0.46	–	0.76	0.10	0.14
$7_1^- \to 5_1^-$	–	2.08	1.91	0.76	–	2.04	1.68	0.39	–	2.74	0.42	0.12
$9_1^- \to 7_1^-$	–	0.01	0.09	0.21	–	0.07	0.02	0.09	–	0.30	0.01	0.04
$11_1^- \to 9_1^-$	–	2.63	2.45	2.23	–	6.79	5.81	3.83	–	7.80	5.08	4.90
$13_1^- \to 11_1^-$	–	0.47	0.30	0.14	–	6.13	5.12	0.76	–	3.74	0.15	0.19
$15_1^- \to 13_1^-$	–	–	–	–	–	5.45	5.07	1.54	–	–	–	–
$17_1^- \to 15_1^-$	–	–	–	–	–	4.01	3.87	2.94	–	–	–	–
μ (μ_N)												
2_1^+	–	−0.140	−0.084	−0.081	–	−0.106	−0.038	−0.068	–	−0.105	−0.018	0.005
4_1^+	–	−0.427	−0.290	−0.359	–	−0.277	−0.362	−0.606	–	−0.571	−0.271	−0.359
6_1^+	–	−0.108	−0.152	−0.186	−0.14(9)	−0.109	−0.163	−0.201	−0.24(12)	−0.024	−0.122	−0.185
8_1^+	–	0.291	−0.117	−0.265	–	−0.158	−0.239	−0.220	–	0.292	−0.212	−0.131
10_1^+	–	−0.061	−0.167	−0.203	–	0.100	−0.114	0.003	–	0.018	−0.124	−0.207
12_1^+	–	–	–	–	–	0.098	−0.077	−0.105	–	–	–	–

In Tables IV and V, we present a few yrast states in terms of their optimized pair basis states, for which corresponding overlaps between the SM wave functions and the optimized pair basis states are larger than 0.8. From Tables IV and V, one sees that the configurations of the positive-parity pair states with $J > 6$ and negative-parity pair states with $J > 9$ are constructed by breaking one or two S pairs of the 6_1^+ and 9_1^- states, which are seniority-two and spin-maximum. This is very similar to the situation of the positive-parity yrast states with $J > 10$, and the negative-parity yrast states with $J > 7$, for the ^{128,126}Sn nuclei.

In Table VI we present our calculated $B(E2)$ values and magnetic moments of ^{104,106,108}Sn, given by the SM, NPA, and optimized pair basis states, and compare them with experimental data. The effective charge for valence neutrons is taken as the opposite of that for neutron holes, namely $e_\nu = 0.88e$; the orbital and spin gyromagnetic ratios for valence neutrons are the same as those for neutron holes. Unfortunately, the enhanced $B(E2,2_1^+ \to 0_1^+)$ values of ^{104,106,108}Sn reported in experiments are not reproduced in any of these calculations assuming the effective charge $e_\nu = 0.88e$ for valence neutrons. In Ref. [12] this systematic deviation was attributed to the large difference between effective charge for the beginning of the 50–82 shell and that for the end of the same shell.

IV. SUMMARY

In this paper we study energy levels and electromagnetic properties of yrast states for semimagic ^{128,126,124}Sn and ^{104,106,108}Sn, by using the monopole-optimized effective interactions based on the realistic CD-Bonn nucleon-nucleon potential, within the frameworks of the nucleon-pair approximation (NPA) and the shell model (SM). For ^{128,126,124}Sn (or ^{104,106,108}Sn), the NPA configuration space for positive parity is constructed by using a few collective neutron-hole pairs (or neutron pairs) with positive parity and even spin, and the configuration space for negative parity is constructed by coupling the positive-parity pairs to one negative-parity pair. It is shown that, for most yrast states in ^{128,126}Sn and ^{104,106}Sn, the overlaps between the wave functions obtained in the full SM space and those obtained in the above truncated space are close to 1.

Very interestingly, we find that many yrast states, not only the well-known seniority-zero ground states and seniority-two states, but also seniority-four and seniority-six states of these nuclei, are well represented by *one-dimensional, optimized pair basis states*. It would be interesting to study whether or not this simple patterns are robust for nonyrast states in these nuclei. Furthermore, a simple hierarchical structure is also observed. For ^{128,126}Sn, the positive-parity yrast states with spin $J > 10$ are well described by breaking one or two S pairs of the 10_1^+ state which is seniority-two, spin-maximum, and positive-parity; similarly, the negative-parity yrast states with spin $J > 7$ are well represented by breaking one or two S pairs of the 7_1^- state which is also seniority-two and spin-maximum but negative-parity. Similar hierarchy is noticed in yrast states of ^{104,106}Sn.

For ^{128,126,124}Sn, according to the occupancies of single-j orbits in the SM wave functions of low-lying yrast states, neutron holes predominantly occupy the $s_{1/2}$, $d_{3/2}$, and $h_{11/2}$ orbits (or the pseudo-"$17/2^-$" orbit of Ref. [11]). Together with the pair configuration of the SM wave function, the evolution of the $B(E2)$ values of the SM calculations with mass number A are explained in terms of the seniority scheme. The $B(E2)$ values of the seniority-changed ($\delta_\nu = 2$) $2_1^+ \to 0_1^+, 12_1^+ \to 10_1^+, 9_1^- \to 7_1^-$ transitions increase as mass number A decreases, while the $B(E2)$ values of the seniority-conserved ($\delta_\nu = 0$) $10_1^+ \to 8_1^+, 7_1^- \to 5_1^-, 15_1^- \to 13_1^-$ transitions decrease and nearly vanish at ^{124}Sn.

ACKNOWLEDGMENTS

We thank the National Natural Science Foundation of China (Grant Nos. 11225524, 11505113), the 973 Program of China (Grant No. 2013CB834401), Shanghai Key Laboratory of Particle Physics and Cosmology (Grant No. 11DZ2260700), the Program of Shanghai Academic/Technology Research Leader (Grant No. 16XD1401600), and China Postdoctoral Science Foundation (Grant No. 2015M580319) for financial support. One of the authors (C.Q.) thanks the Swedish Research Council (VR) (Grants No. 621-2012-3805, No. 621-2013-4323), and the Göran Gustafsson foundation. This work is also supported by the Center for High Performance Computing (HPC) at Shanghai Jiao Tong University. The shell-model calculations for ^{124}Sn and ^{108}Sn are performed on resources provided by the Swedish National Infrastructure for Computing (SNIC) at PDC, KTH, Stockholm.

[1] A. Banu, J. Gerl, C. Fahlander *et al.*, Phys. Rev. C **72**, 061305(R) (2005).
[2] J. Cederkäll, A. Ekström, C. Fahlander *et al.*, Phys. Rev. Lett. **98**, 172501 (2007).
[3] C. Vaman, C. Andreoiu, D. Bazin *et al.*, Phys. Rev. Lett. **99**, 162501 (2007).
[4] A. Ekström, J. Cederkäll, C. Fahlander *et al.*, Phys. Rev. Lett. **101**, 012502 (2008).
[5] P. Doornenbal, P. Reiter, H. Grawe *et al.*, Phys. Rev. C **78**, 031303(R) (2008).
[6] G. Guastalla, D. D. DiJulio, M. Górska *et al.*, Phys. Rev. Lett. **110**, 172501 (2013).
[7] V. M. Bader, A. Gade, D. Weisshaar *et al.*, Phys. Rev. C **88**, 051301(R) (2013).
[8] P. Doornenbal, S. Takeuchi, N. Aoi *et al.*, Phys. Rev. C **90**, 061302(R) (2014).
[9] T. Bäck, C. Qi, B. Cederwall *et al.*, Phys. Rev. C **87**, 031306(R) (2013).
[10] L. Coraggio, A. Covello, A. Gargano, N. Itaco, and T. T. S. Kuo, Phys. Rev. C **91**, 041301(R) (2015).
[11] I. O. Morales, P. V. Isacker, and I. Talmi, Phys. Lett. B **703**, 606 (2011).
[12] H. Jiang, Y. Lei, G. J. Fu, Y. M. Zhao, and A. Arima, Phys. Rev. C **86**, 054304 (2012).

[13] J. M. Allmond, A. E. Stuchbery, A. Galindo-Uribarri *et al.*, Phys. Rev. C **92**, 041303(R) (2015).
[14] C. T. Zhang, P. Bhattacharyya, P. J. Daly, Z. W. Grabowski, R. Broda, B. Fornal, and J. Blomqvist, Phys. Rev. C **62**, 057305 (2000).
[15] N. Fotiades, M. Devlin, R. O. Nelson *et al.*, Phys. Rev. C **84**, 054310 (2011).
[16] S. Pietri, A. Jungclaus, M. Górska *et al.*, Phys. Rev. C **83**, 044328 (2011).
[17] A. Astier, M.-G. Porquet, Ch. Theisen *et al.*, Phys. Rev. C **85**, 054316 (2012).
[18] Ł. W. Iskra, R. Broda, R. V. F. Janssens *et al.*, Phys. Rev. C **89**, 044324 (2014).
[19] R. Broda, R. H. Mayer, I. G. Bearden *et al.*, Phys. Rev. Lett. **68**, 1671 (1992).
[20] D. C. Radford, C. Baktash, J. R. Beene *et al.*, Nucl. Phys. A **746**, 83c (2004).
[21] A. Jungclaus, J. Walker, J. Leske *et al.*, Phys. Lett. B **695**, 110 (2011).
[22] J. Walker, A. Jungclaus, J. Leske *et al.*, Phys. Rev. C **84**, 014319 (2011).
[23] J. M. Allmond, D. C. Radford, C. Baktash *et al.*, Phys. Rev. C **84**, 061303(R) (2011).
[24] J. M. Allmond, A. E. Stuchbery, D. C. Radford *et al.*, Phys. Rev. C **87**, 054325 (2013).
[25] I. Talmi, Nucl. Phys. A **172**, 1 (1971).
[26] S. Shlomo and I. Talmi, Nucl. Phys. A **198**, 81 (1972).
[27] I. Talmi, *Simple Models of Complex Nuclei* (Harwood Academic Press, Chur, Switzerland, 1993).
[28] Y. K. Gambhir, A. Rimini, and T. Weber, Phys. Rev. **188**, 1573 (1969).
[29] K. Allart, E. Boeker, G. Bonsignori, M. Saroia, and Y. K. Gambhir, Phys. Rep. **169**, 209 (1988).
[30] N. Sandulescu, J. Blomqvist, T. Engeland, M. Hjorth-Jensen, A. Holt, R. J. Liotta, and E. Osnes, Phys. Rev. C **55**, 2708 (1997).
[31] D. J. Dean and M. Hjorth-Jensen, Rev. Mod. Phys. **75**, 607 (2003).
[32] M. P. Kartamyshev, T. Engeland, M. Hjorth-Jensen, and E. Osnes, Phys. Rev. C **76**, 024313 (2007).
[33] M. A. Caprio, F. Q. Luo, K. Cai, V. Hellemans, and Ch. Constantinou, Phys. Rev. C **85**, 034324 (2012).
[34] Y. M. Zhao and A. Arima, Phys. Rep. **545**, 1 (2014), and references therein.
[35] C. Qi and Z. X. Xu, Phys. Rev. C **86**, 044323 (2012).
[36] R. Machleidt, Phys. Rev. C **63**, 024001 (2001).
[37] M. Hjorth-Jensen, T. T. S. Kuo, and E. Osnes, Phys. Rep. **261**, 125 (1995).
[38] J. Q. Chen, Nucl. Phys. A **626**, 686 (1997).
[39] Y. M. Zhao, N. Yoshinaga, S. Yamaji, J. Q. Chen, and A. Arima, Phys. Rev. C **62**, 014304 (2000).
[40] G. J. Fu, Y. Lei, Y. M. Zhao, S. Pittel, and A. Arima, Phys. Rev. C **87**, 044310 (2013).
[41] http://www.nndc.bnl.gov/ensdf/.